Zahn, R., Comas, M.C., and Klaus, A. (Eds.), 1999
Proceedings of the Ocean Drilling Program, Scientific Results, Vol. 161

22. Ar-Ar DATING OF BIOTITE AND MUSCOVITE FROM ALBORAN BASEMENT SAMPLES, SITE 976[1]

S.P. Kelley[2] and J.P. Platt[3]

ABSTRACT

Ar-Ar dating of muscovite and biotite from high-grade schist and pelitic gneiss cored at Ocean Drilling Program Site 976 in the Alboran Sea yield cooling ages in the range 18.5 to 20 Ma. The difference in mean age of the two minerals is only 0.8 ± 0.5 Ma, indicating cooling through the range of closure temperatures of these minerals (426°–330°C) at between 75° and 320°C per m.y. during the early Miocene. The Ar-Ar ages are very close to the apatite fission track ages reported from the same rocks, requiring overall cooling rates of the order of 150°C/m.y., and a minimum exhumation rate of 2.5 km/m.y. The mean muscovite age (20.0 ± 0.2 Ma) is ~1 m.y. older than muscovite Ar-Ar ages reported from high-grade metamorphic basement in the adjacent Betic Cordillera of southern Spain. This implies that there was a regional thermal event across much of the Alboran region, but that small differences in cooling age may be detectable. The thermal event, and the subsequent rapid exhumation of the metamorphic basement, coincide in time with the extensional tectonic event that created the Alboran Sea basin, suggesting a causal link between these processes.

INTRODUCTION

The Alboran Sea is an extensional basin of late Tertiary age that formed in close association with the Betic-Rif thrust belt in adjacent regions of southern Spain and Morocco. The Ocean Drilling Program (ODP) established during Leg 161 that the basement underlying the Neogene sediments of the basin is made up of high-grade metamorphic rocks closely comparable to those found in adjacent regions of the Betic Cordillera (Shipboard Scientific Party, 1996). This appears to confirm the hypothesis that the Alboran Sea has formed by the rapid extensional collapse of an earlier collisional orogen that occupied the region (Platt and Vissers, 1989). The thermal evolution of these rocks is therefore of crucial importance to understanding the timing and mechanism of basin formation. Platt et al. (1996) have reported that the basement rocks cored at Site 976 show evidence of decompression from a metamorphic pressure of 8 kb or more, and that decompression was accompanied by an increase in temperature to ~650° to 700°C at low pressure. This paper reports on the results of postcruise Ar-Ar dating of basement core samples, which provide the first constraints on the timing of the thermal event recorded in these rocks.

GEOLOGICAL SETTING

ODP Site 976 is located on a buried basement high in the west Alboran Basin that was defined by normal faulting, probably in early to middle Miocene time (Comas et al., 1992; Watts et al., 1993). The crustal thickness in the area is probably between 15 and 20 km. The basement is covered unconformably by 670 m of sediment of Serravallian (middle Miocene) to Pleistocene age (Shipboard Scientific Party, 1996), which places a younger age limit of about 13 Ma on the exhumation of the metamorphic rocks.

In Hole 976B, the top 124 m of the basement core consists of high-grade pelitic schist, with interlayers of calcite and dolomite marble and associated calc-silicate rock. The bulk of the rock consists of quartz-biotite-sillimanite-plagioclase-K-feldspar schist, with porphyroblasts of garnet, staurolite, and andalusite. This passes down into a massive pelitic gneiss, which is locally migmatitic, with irregular veins and segregations of granitic material. The gneiss carries abundant cordierite, sillimanite, and andalusite in addition to quartz, biotite, and two feldspars. Muscovite is present as a late-stage hydrothermal mineral in veins, and as an alteration product of aluminosilicate minerals and cordierite. Both the schist and the gneiss are cut by leucogranitic dikes, as well as numerous zones of brittle fault gouge and breccia. The petrology of both rock types suggests that they reached peak temperatures in the range of 650°C to 700°C at pressures of 3±5 kb (Platt et al., 1996; Shipboard Scientific Party, 1996; Soto et al., Chap. 19, this volume; Soto et al., unpubl. data).

SAMPLE DESCRIPTION

Four samples were selected from Hole 976B basement core for Ar-Ar analysis: one sample of high-grade schist from near the top of the basement, one sample of migmatitic gneiss from near the contact with the overlying high-grade schist, and two further samples of migmatitic gneiss from near the bottom of the hole.

Sample 161-976B-76R-2 (Piece 4), of high-grade schist, contains coarse-grained biotite that appears to have reached textural equilibrium with a late-stage mineral assemblage including plagioclase, K-feldspar, and andalusite. Sillimanite and corundum crystallized somewhat earlier. The late-stage assemblage is likely to have formed at about 600°C and 2 kb pressure (Soto et al., unpubl. data), above the stability limit of muscovite (accounting for the absence of this mineral).

Four samples of migmatitic gneiss were analyzed: Samples 161-976B-95R-1 (Piece 14B), 101R-1 (Piece 9), 102R-1 (Piece 10), and 102R-2 (Piece 10B). All four contain quartz, plagioclase, K-feldspar, biotite, muscovite, andalusite, sillimanite, cordierite, Fe-oxide, and accessory minerals. The biotite appears to form part of a late assemblage including andalusite and cordierite that probably formed during cooling at about the same time as the granitic leucosome material crystallized. This assemblage probably also crystallized at about

[1]Zahn, R., Comas, M.C., and Klaus, A. (Eds.), 1999. *Proc. ODP, Sci. Results,* 161: College Station, TX (Ocean Drilling Program).
[2]Department of Earth Sciences, The Open University, Walton Hall, Milton Keynes MK7 6AA, United Kingdom. s.p.kelley@oper.ac.uk
[3]Department of Geological Sciences, University College London, Gower Street, London WC1E 6BT, United Kingdom.

600°C and 2 kb (Soto et al., unpubl. data). The muscovite in these rocks is essentially a late alteration product, forming at the expense of andalusite, sillimanite, and cordierite. In Sample 161-976B-101R-1 (Piece 9), coarse-grained muscovite fills a pull-apart structure in the gneiss, and in Sample 102R-1 (Piece 10) it occurs as a vein filled with coarse-grained muscovite obliquely oriented to the vein walls. The late alteration and veining is likely to be related to percolating aqueous fluids residual from the crystallization of the granitic leucosome. If this interpretation is correct, then the likely temperature of crystallization of the muscovite would have been not far below the wet granite solidus, which even allowing for significant content of Al and volatile components such as B, would still be close to 600°C at 2 kb (Soto et al., unpubl. data).

METHODOLOGY

Polished thick sections (less than 0.5 mm) of the Alboran Sea samples were removed from their glass slides and adhesive removed by ultrasonic treatment in methanol and subsequently in deionized water. Samples were then wrapped in aluminum foil, and irradiated in the nuclear reactor at the Oregon State University. Upon return, the samples were loaded into an ultra-high vacuum laser chamber with a kovar window and baked to 120°C overnight to remove adsorbed atmospheric argon from the sample and chamber walls. Samples for argon isotope measurement were extracted from 50–100 µm laser pits using short 10–25 ms pulses from a focused continuous-wave neodymium-yttrium-aluminum-garnet (CW Nd-YAG) laser (Kelley, 1995). Samples were extracted from individual in situ mica grains in thick sections. Where possible, the laser was used to extract one analysis per mica, though, in some cases, they were intimately intergrown. The laser was fired through a Leica Mettalux 3 microscope, which was also used to observe mineral textures during analysis. Active gases were removed using Zr-Al getters and the remaining noble gases equilibrated into an MAP 215-50 static mass spectrometer with a Johnston multiplier detector. Argon isotope peak intensities were measured 10 times in a sequence lasting ~15 min. Peak intensities were extrapolated back to the inlet time and corrected for blanks, mass spectrometer discrimination, and reactor-induced interferences. Mean blank measurements during the experiment for ^{40}Ar, ^{39}Ar, ^{38}Ar, ^{37}Ar and ^{36}Ar, were 6.9, 0.05, 0.03, 1.2, and 0.25×10^{-12} cm^3 STP (standard temperature and pressure), respectively. Two aliquots of the international biotite mineral standard, GA1550 (McDougall and Harrison, 1988), were run adjacent to the unknowns yielding identical J values within acceptable errors. The J value for these samples was 0.005609 ± 0.000028.

Ages were calculated by fitting a line on $^{36}Ar/^{40}Ar$ vs. $^{39}Ar/^{40}Ar$ correlation diagrams using the York (1969) fitting algorithm and errors are quoted at the 2σ level including the error on the J value. This technique yields errors that reflect not only the analytical errors of the analysis, but also the geological scatter caused by heterogeneous alteration of the sample. Thus, altered samples yielded scattered data, often with high atmospheric Ar contents, a high MSWD (mean squared weighted deviation), and high errors on the final age. Most samples produced isochron ages that reflected simple mixtures of radiogenic and atmospheric components though some exhibited excess argon, reflected in intercepts below 0.003384 (the isotope ratio of atmospheric argon) on the $^{36}Ar/^{40}Ar$ axis.

RESULTS

A summary of the Ar-Ar results appears in Table 1, and a full data table is presented as Table 2. Biotite analyses from Sample 161-976B-76R-2 (Piece 4) yielded an isochron age of 19.0 ± 0.4 Ma, an atmospheric intercept and an MSWD of 2.0 (Fig. 1A). Coexisting muscovite and biotite in Sample 95R-1 (Piece 14B) yielded ages of 18.5 ± 0.4 Ma with an MSWD of 0.7 (Fig. 1B) and 20.1 ± 0.4 Ma with an MSWD of 1.2 (Fig. 1C). Intercepts were forced through the atmospheric ratio though this makes little difference to the ages. Muscovite from Sample 161-976B-101R1-9 (which occurs in a cross-cutting vein) yielded an age of 19.9 ± 0.6 Ma, an MSWD of 1.2, and a $^{36}Ar/^{40}Ar$ intercept value of 0.00438 ± 0.0096 ($^{40}Ar/^{36}Ar$ = 228 ± 50) a value below that for atmospheric argon (Fig. 1D). However, the value is within 2 ó errors of the atmospheric value and possibly reflects mixing between true muscovite analyses and slightly altered, low potassium/high atmospheric argon analyses. Biotite analyses from Sample 102R-1 (Piece 10) do not yield an isochron and reflect the introduction of excess argon with variable ratios around 800. Biotite analyses from Sample 102R-2 (Piece 10B) yielded an isochron age of 20.1 ± 0.6 Ma, an intercept value of 0.0018 ± 0.00008 ($^{40}Ar^{36}Ar$ = 555 ± 25), and an MSWD of 0.6.

Table 1. Ages calculated from isochron plots.

Sample	Mineral	Age	2 σ error
161-976B-			
76R-2 (Piece 4)	Biotite	19	0.4
95R-1 (Piece 14B)	Biotite	18.5	0.4
95R-1 (Piece 14B)	Muscovite	20.1	0.4
101R-1 (Piece 9)	Muscovite	19.9	0.6
101R-1 (Piece 10)	Muscovite and Biotite	—	Excess argon
102R-2 (Piece 10B)	Biotite	20.1	0.6

Within the 215 m vertical distance separating the samples, age variations are greater than the analytical uncertainty, but as Figure 2 shows, the distribution of muscovite and biotite Ar-Ar ages with depth below the sediment/basement interface exhibits no obvious correlation with depth. This result corroborates apatite fission track ages from Site 976 (Hurford et al., Chap. 21, this volume), which show no correlation with depth at the same site. The difference between ages of co-existing muscovite and biotite is 1.6 ± 0.6 Ma, though it is difficult to derive a reliable cooling estimate from one pair of ages. Given the lack of age/depth correlation in either the fission track or Ar-Ar ages, a more reliable estimate comes from the difference between the mean ages for the borehole samples: 20.0 ± 0.2 Ma for muscovite and 19.2 ± 0.7 Ma for biotite. Although these numbers represent only a small population of samples, a mean age difference of 0.8 ± 0.5 Ma implies rapid cooling.

Although the error on the age difference is high, it is possible to place constraints upon the cooling rate by calculating the closure temperatures for muscovite and biotite. Closure temperatures were calculated using the standard equation of Dodson (1973). The mica grain sizes used were measured in thin section and were close to 200 µm for all the samples analyzed here, except for muscovite in Sample 101R-1 (Piece 9), which has a grain size of around 700 µm. Cooling rates of 100°C were used, as they are known to be of this order, and as variations of 50–100°C about this number make little difference to the derived temperatures. Closure temperatures of 330°C for biotite (using the diffusion parameters of Grove and Harrison, 1996) and 404°–449°C (mean = 426°C) for muscovite (using the diffusion parameters of Hames and Bowring, 1994). The absolute numbers are maximum values given that the effective grain sizes may be reduced by internal cracks or defects within the micas, but by using both micas the effect may be reduced, as both micas will suffer similar effects. The mica closure temperatures thus indicate cooling rates of between 75°C and 320°C per Ma for Site 976.

Comparisons between the borehole samples from Site 976 and land-based samples in the western Betic Cordilleras reported by Zeck et al. (1992) and Monié et al. (1994) illustrate the variation across the basin. Figure 3A shows gaussian distributions of muscovite ages from Site 976 and the western Betic Cordilleras indicating narrow age populations that are very reproducible from site-to-site on land and are all around 1 m.y. younger than the ages derived from Site

Table 2. Ar-Ar data for muscovite and biotite single-spot ages.

Sample 161-976B-	Mineral	$^{40}Ar/^{39}Ar$	$^{38}Ar/^{39}Ar$	$^{37}Ar/^{39}Ar$	$^{36}Ar/^{39}Ar$	^{39}Ar#	$^{40}Ar^*/^{39}Ar$	Age (Ma)*	1σ error
76R-2 (Piece 4)									
1	Biotite	1.883	0.052	0.0075	0.0008	15.6	1.65	16.6	1.2
2	Biotite	2.027	0.047	0.0018	0.0003	126.7	1.93	19.4	0.3
3	Biotite	1.975	0.047	0.0015	0.0002	111.0	1.93	19.4	0.3
4	Biotite	1.998	0.050	0.0028	0.0007	46.4	1.78	18.0	0.5
5	Biotite	1.953	0.050	0.0034	0.0005	61.1	1.81	18.2	0.4
6	Biotite	2.028	0.051	0.0004	0.0001	64.1	1.99	20.0	0.4
7	Biotite	1.985	0.050	0.0003	0.0002	54.2	1.94	19.5	0.5
8	Biotite	2.358	0.050	0.0014	0.0010	74.7	2.08	20.9	0.4
9	Biotite	2.048	0.045	0.0025	0.0009	52.4	1.79	18.0	0.4
10	Biotite	2.073	0.047	0.0031	0.0008	69.2	1.84	18.5	0.5
11	Biotite	1.868	0.048	0.0032	0.0003	46.0	1.79	18.0	0.7
95R-1 (Piece 14B)									
1	Muscovite	2.662	0.021	0	0	18.1	2.80	28.1	1.1
2	Muscovite	2.279	0.020	0.0006	0.0007	50.0	2.08	20.9	0.5
3	Muscovite	2.082	0.018	0.0003	0.0003	181.8	1.99	20.1	0.2
1	Biotite	2.021	0.019	0.0011	0.0006	58.6	1.85	18.6	0.6
4	Muscovite	2.024	0.017	0	0.0001	103.1	2.00	20.1	0.3
5	Muscovite	1.997	0.019	0.0007	0.0003	49.7	1.92	19.3	0.6
2	Biotite	1.978	0.018	0.0016	0.0006	40.2	1.79	18.1	0.5
3	Biotite	1.983	0.018	0.0003	0.0004	103.2	1.85	18.6	0.3
4	Biotite	1.962	0.019	0.0012	0.0005	76.7	1.82	18.3	0.3
6	Muscovite	2.102	0.019	0.0009	0.0004	105.4	1.97	19.9	0.4
101R-1 (Piece 9)									
1	Muscovite	2.358	0.026	0.0045	0.0012	26.7	1.80	18.1	2.1
2	Muscovite	2.191	0.022	0.0012	0.0008	52.0	1.95	19.7	0.6
3	Muscovite	2.137	0.020	0.0016	0.0008	54.2	1.84	18.5	0.6
4	Muscovite	2.107	0.021	0.0035	0.0006	48.1	1.75	17.6	1.0
5	Muscovite	2.061	0.018	0.0005	0.0003	83.1	1.97	19.8	0.3
6	Muscovite	2.057	0.020	0.0013	0.0006	134.2	1.88	18.9	0.4
7	Muscovite	2.019	0.018	0.0003	0.0002	116.8	1.97	19.8	0.3
8	Muscovite	1.994	0.018	0.0003	0.0001	72.0	1.91	19.2	0.5
102R-1 (Piece 10)									
	Muscovite	3.538	0.024	0.0009	0.0024	56.7	2.84	28.5	0.6
1	Biotite	3.534	0.019	0	0.0013	47.6	3.14	31.5	0.8
2	Biotite	2.707	0.029	0.0005	0.0015	37.6	2.28	22.9	0.8
2	Muscovite	2.705	0.018	0	0.0012	82.2	2.36	23.7	0.5
3	Muscovite	2.602	0.022	0.0008	0.0013	69.6	2.23	22.4	0.5
4	Muscovite	2.521	0.017	0.0004	0.0006	39.7	2.33	23.5	0.6
5	Muscovite	2.490	0.015	0.0011	0.0003	29.4	2.41	24.2	1.0
3	Biotite	2.398	0.026	0	0.0006	40.2	2.21	22.3	0.6
4	Biotite	2.235	0.023	0.0031	0.0020	21.3	1.65	16.6	1.4
5	Biotite	1.990	0.020	0.0009	0.0006	91.3	1.81	18.3	0.3
102R-2 (Piece 10B)									
1	Biotite	7.429	0.074	0.0006	0.0100	34.2	4.49	44.8	1.6
2	Biotite	3.015	0.033	0.0008	0.0018	61.9	2.47	24.9	0.7
3	Biotite	2.951	0.031	0.0005	0.0012	55.8	2.59	26.1	0.7
4	Biotite	2.550	0.028	0.0005	0.0009	102.1	2.27	22.8	0.4
5	Biotite	2.477	0.025	0.0009	0.0009	39.8	2.20	22.1	1.0
6	Biotite	2.422	0.016	0.0004	0.0002	40.9	2.36	23.7	0.8
7	Biotite	2.301	0.023	0.0015	0.0005	55.8	2.17	21.8	0.4
8	Biotite	2.234	0.022	0.0008	0.0004	38.5	2.10	21.2	0.6
9	Biotite	2.225	0.020	0.0007	0.0005	95.6	2.07	20.8	0.4
10	Biotite	2.185	0.027	0.0007	0.0004	78.7	2.08	20.9	0.4

Notes: * = J value = 0.005609 ± 0.000028. # = ^{39}Ar amounts in 10^{-12} cm^3 STP

976. Figure 3B illustrates the same distribution for the biotite ages. This shows a much higher degree of scatter, and both land-based and borehole samples range from 18.5 to 20.5 Ma with no obvious correlation between age and position. It seems likely that the Ar-Ar ages for biotites have been more affected by problems of excess argon and argon loss in both borehole and land-based samples.

TECTONIC IMPLICATIONS

The Ar-Ar data on muscovite and biotite suggest relatively rapid cooling of the basement rocks through the closure temperature range of these two minerals (330°–426°C) between 18.5 and 20.5 Ma. Taken together with the fission-track evidence from the same rocks (Hurford et al., Chap. 21, this volume), indicating cooling to 60°C at ~8–19 Ma, it is clear that the basement cooled from 450°C to 60°C in 2.5 m.y. or less, a cooling rate of over 150°C/m.y. This is confirmed by the muscovite/biotite age separation of only 0.8 ± 0.5 m.y, implying cooling rates of 75° to 320°C/m.y. Conversion of the cooling rate into an exhumation rate requires assumptions about the thermal gradient, and is complicated by the fact that rapid exhumation causes significant advection of heat toward the earth's surface, steepening the geotherm. Platt et al. (unpubl. data) have carried out numerical modeling of the exhumation path in order to investigate these effects. Taking the PT estimate by Soto et al. (unpubl. data) of 650°C and 3.5 kb for the thermal peak of metamorphism, the presently exposed rocks would need to be exhumed from these conditions at a rate of 2.5 km/m.y. to produce cooling from 420° to 60°C in 2.5 m.y. During this process the near-surface thermal gradient would increase from 50°C/km to about 90°C/km. This is, therefore, a minimum rate of exhumation: if we assume a more normal orogenic thermal gradient of 30°C/km, the exhumation rate required would be 5 km/m.y.

The Ar-Ar cooling ages from Site 976 are very similar to those reported from similar high-grade metamorphic basement in the Betic Cordillera nearby in southern Spain (Zeck et al., 1992; Monié et al., 1994) only 80 km northwest of Site 976. Although biotite ages are somewhat scattered, it seems from our preliminary data that muscovite ages are an average of 1 m.y. older at Site 976. The difference,

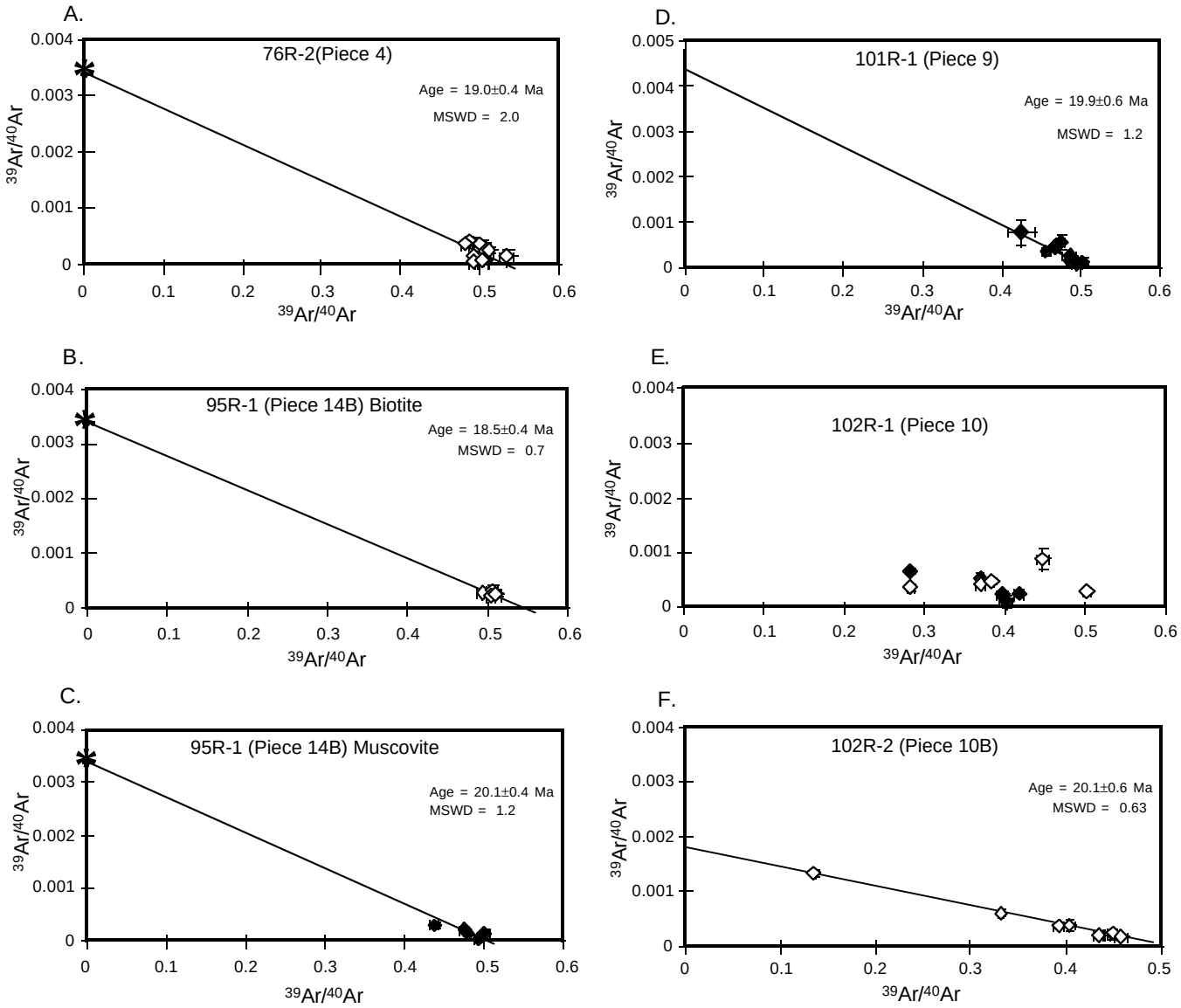

Figure 1. **A–F.** Isochron diagrams for muscovite and biotite in basement samples from Site 976. Muscovite shown as closed symbols and biotite as open symbols in (E).

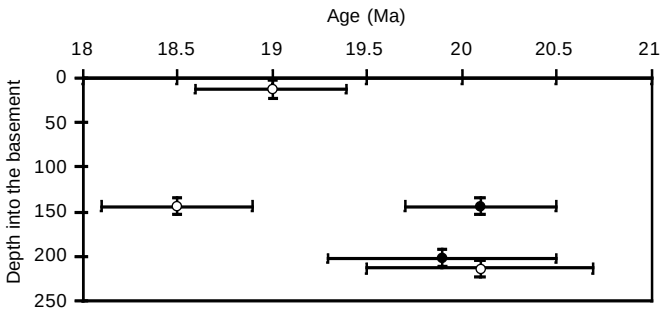

Figure 2. The relationship between depth and Ar-Ar age for muscovite and biotite samples. Muscovite shown as closed circles, biotite shown as open circles.

though small, may be very significant in detecting the underlying mechanism causing the rapid cooling and will be the subject of further study, though it is now possible to say that these ages reflect a regional thermal event of early Miocene age. In view of the fact that parts of the west Alboran basin contain early Miocene sediments that may be as old as the late Aquitanian (about 20 Ma; Comas et al., 1992), there appears to be a very close link between this thermal event and the subsequent rapid exhumation and the initiation of the Alboran Sea Basin. The phase of extensional tectonics that created the Alboran Sea provides a mechanism for the rapid exhumation of the metamorphic basement, and the thermal event may reflect changes in the structure of the underlying lithosphere that caused the extensional event (Platt and Vissers, 1989; Platt and England, 1994).

ACKNOWLEDGMENTS

Funded by grant number GR3/10828 from the Natural Environmental Research Council of Great Britain.

REFERENCES

Comas, M.C., García-Dueñas, V., and Jurado, M.J., 1992. Neogene tectonic evolution of the Alboran Basin from MCS data. *Geo-Mar. Lett.*,12:157–164.

Dodson, M., 1973. Closure temperature in cooling geochronological and petrological systems. *Contrib. Mineral. Petrol.*, 40:259–274.

Grove, M., and Harrison, T.M., 1996. $^{40}Ar^*$ diffusion in Fe-rich biotite. *Am. Mineral.*, 81:940–951.

Hames, W.E., and Bowring, S.A., 1994. An empirical evaluation of the argon diffusion geometry in muscovite. *Earth Planet. Sci. Lett.*, 124:161–167.

Kelley, S.P., 1995. The laser microprobe Ar-Ar technique of dating. *In* Potts, P.J., Bowks, J.F.W., Reed, S.J.B., and Cave, M.R. (Eds.), *Microprobe Techniques in the Earth Sciences:* London (Chapman and Hall), 326–358.

McDougall, I., and Harrison, T.M., 1988. *Geochronology and Thermochronology by the $^{40}Ar/^{39}Ar$ Method:* New York (Oxford Univ. Press).

Monié, P., Torres-Roldan, R.L., and Garcia-Casco, A., 1994. Cooling and exhumation of the western Betic Cordilleras, $^{40}Ar/^{40}Ar$ thermochronological constraints on a collapsed terrane. *Tectonophysics*, 238:353–379.

Platt, J.P., and England, P.C., 1994. Convective removal of lithosphere beneath mountain belts: thermal and mechanical consequences. *Am. J. Sci.*, 294:307–336.

Platt, J.P., and Vissers, R.L.M., 1989. Extensional collapse of thickened continental lithosphere: a working hypothesis for the Alboran Sea and Gibraltar Arc. *Geology*, 17:540–543.

Platt, J.P., Soto, J.I., Comas, M.C., and Leg 161 Shipboard Scientists, 1996. Decompression and high-temperature-low-pressure metamorphism in the exhumed floor of an extensional basin, Alboran Sea, western Mediterranean. *Geology*, 24:447–450.

Shipboard Scientific Party, 1996. Site 976. *In* Comas, M.C., Zahn, R., Klaus, A., et al., *Proc. ODP, Init. Repts.*, 161: College Station, TX (Ocean Drilling Program), 179–297.

Watts, A.B., Platt, J.P., and Buhl, P., 1993. Tectonic evolution of the Alboran Sea Basin. *Basin Res.*, 5:153–177.

York, D., 1969. Least-squares fitting of a straight line with correlated errors. *Earth Planet. Sci. Lett.*, 5:320–324.

Zeck, H.P., Monié, P., Villa, I.M., and Hansen, B.T., 1992. Very high rates of cooling and uplift in the Alpine belt of the Betic Cordilleras, southern Spain. *Geology*, 20:79–82.

Date of initial receipt: 23 April 1997
Date of acceptance: 1 October 1997
Ms 161SR-215

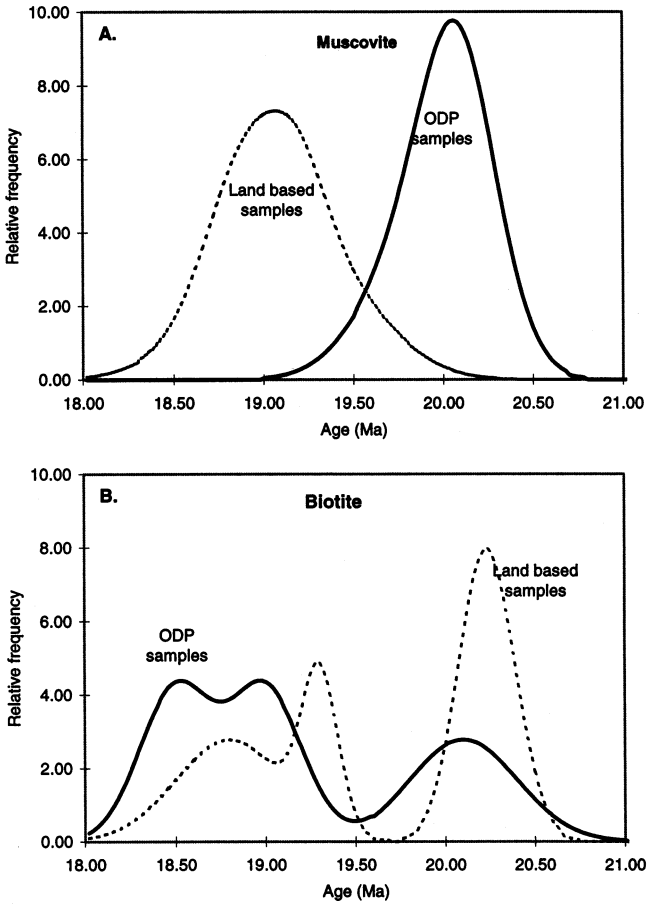

Figure 3. Age populations for (**A**) muscovite and (**B**) biotite illustrating the relationship between samples obtained from Site 976 and those on land to the north. These population spreads were produced by summing gaussian error distributions.